LARGE BONE TUMOUR DEFECTS: PERSONALISED SHAPE RECONSTRUCTION AND PLATE DESIGN

F. GELAUDE*, J. VANDER SLOTEN* and B. LAUWERS**

* Division of Biomechanics and Engineering Design, K.U.Leuven, Heverlee, Belgium
** Division Production, Machine Design and Automation, K.U.Leuven, Heverlee, Belgium

frederik.gelaude@mech.kuleuven.be

Abstract: Bone defects, tumours or malformations occur for different bone types. They are treated surgically by removing and reconstructing the affected bone region. Stable reconstructions of large vulnerable openings in the bone cortex can be attained by the use of thin preformed titanium plates, also denoted 'membranes'. The clinical applicability of these implants has been demonstrated; first the shape is assessed and then an appropriate production technique is applied. Current reconstruction techniques such as clay modelling and a layer-by-layer, Boolean or freeform CAD approach are effective, but still require much manual input. Starting from a developed filter and mesh generating procedure, this paper describes the methodology to more automatically reconstruct the anatomical shape of bone tumour defects, to subsequently extract a plate from the reconstructed surface mesh, and to adjust the plate design to a particular production technique.

Introduction

Bone tumours frequently occur in the upper extremity, such as in the proximal humerus, distal radius and phalanges of the hand, and in the lower extremity, such as in the proximal and distal femur. The surgical treatment of most tumours is a two-stage procedure. First the tumour is removed and controlled, and then the defect is reconstructed. For the former task, the surgeon disposes of several curettage and tumour control procedures, which must be performed very precisely to decrease the recurrence rate [1][2]. For the second task, the bone cavity which originates from removing the tumour must be filled with a particular material, in order to restore the structural integrity and the function of the bone. Additionally, large defects may require a osteosynthesis technique to reinforce the defect reconstruction [2]. Preformed and custom-made titanium membranes (thin metal plate), which are screwed onto the periosteal side of the bone are valid equipment to restore the mechanical strength of the bone and to contain the used filling materials [2]. In addition to applications of tumour reconstructive surgery, titanium membranes are already succesfully applied in maxillo-facial surgery, namely titanium cranioplasties [3], mandibular reconstruction and bone augmentations [4].

The application field of personalised implants such as titanium membranes, can be broadened if their clinical outcome is equal or improved with respect to standardised equipment, if a significant reduction in surgery duration is obtained, and if these implants are rapidly available for a reasonable price. A solution to these requirements includes an efficient and automated design environment which develops personalised titanium membranes for multiple types of bone defects, thereby enabling a streamlined production. Current shape reconstruction techniques, either with modelling clay and spatulas in a lab, in a layer-by-layer or Boolean CAD approach [2][5], or in a specialised software environment [3Matic®][ProEngineer®] are highly effective but still require much manual input and focus mainly on the design.

This paper describes the methodology to more automatically reconstruct the anatomical shape of bone tumour defects, and the subsequent plate extraction from the reconstructed bone surface mesh. Additionally, possibilities are implemented to smooth particular plate regions, and to emphasize the plate outline according to a particular production technique.

Since an appropriate representation of the outer bone cortex is required to design a surface based implant, the segmentation technique used for the plate design in this paper consists of a straightforward grey level segmentation followed by a general filter, as previously developed by the author [6]. The extended filter procedure only retains contour information representing the outer cortex. The developed medical image based design methodology can then either convert a contour set of a specific bone type, e.g. femur or tibia, to an outer bone cortex triangulation mesh or vice versa. These model characteristics enable straightforward and moreover accurate shape reconstructions of various bone defects, which for example originate from a bone tumour. Finally, the reconstructed personalized outer cortex mesh is used to deduce surface based reconstruction plates, also denoted membranes. The complete methodology of automated bone reconstructions is illustrated by means of two bone tumour simulation cases, more specific by a proximal tibia and a bulging distal femur tumour. For the first case, the filter procedure suffices, while the latter requires a more extended approach. All developed procedures are implemented in Matlab®.

IFMBE Proc. 2005 11(1)
ISSN: 1727-1983

Materials and Methods

The bone contours are extracted from the patients CT-data by a quick grey value segmentation in a commercial software, such as Mimics®. Then, an extended semi-automated filter procedure, which is implemented in Matlab®, only retains contour information representing the outer cortex as more specific internal contours, internal loops and shape irregularities are removed, tailoring the image for the above-mentioned application. The removal of the internal loops is thereby of particular interest; full detail on other aspects of the developed filter methodology is available elsewhere [6].

If the bone cortex has a small opening, a large internal loop is formed. The procedure seeks for start and endpoints which are less than a certain distance from one another, but enclose more than a specific amount of points. In every iteration step, the loop with the largest enclosed area is removed and corrected by inserting points between start and endpoint ('1st variant').

Especially when processing bone defects, wide open U-shaped internal loops may appear in the contours. As this information is undesirable for membrane based reconstructions, it must be removed from the set. With this in view, two more variants on the procedure that removes internal loops are implemented. They vary the parameter settings, namely the distance between the start and endpoints of a loop and the area in which these points may reside, and in contrast to the first variant, the procedure only removes the largest loop. The second variant therefore calculates for every segment of the polyline the angle with the horizontal axis. If the range of the least squares lines in the cumulative angle diagram of a contour is small, large internal loops are expected with about halve the contours perimeter (Figure 1c). The loop removal procedure is then executed with no distance or position limitation for the points in a pair and is halted after removing the largest loop. A third variant is implemented to search open cortices in a constrained search area, without any restriction on the distance between start and endpoints. To define the search area and the contours to investigate, the user either indicates a search region on a three dimensional visualisation mesh of the bone or a fixed search area on the global grid in caudal-cranial view.

Finally, a triangulated *outer* surface mesh is built from the spline set, which is created from the contours by the filter procedure.

Applying the filters on a contour set with a middle-sized hole automatically leads to a reconstruction of the tumour hole.

Applying the filters on a bulging bone tumour efficiently cleans up the data but maintains the defect in the mesh. An additional reconstruction procedure therefore loads the contour sets of the tumour bone and the mirrored intact contralateral bone piece. Tumour contours are categorized as 'bulging' by comparing the perimeters and the enclosed surfaces with those from the corresponding intact contours (Figure 2b). A matching procedure, more specific the Iterative Closest Point algorithm (Besl & McKay, 1992) is applied to match the healthy part of each bulging contour with the complete intact contour (Figure 2c, left). The healthy part is known since the user once indicates the overall grid rectangles in caudal-cranial view in which the tumour is present; these regions are scaled according to the contour envelopes. Each bulging contour, for which two appropriate crossovers with the corresponding intact contour could be selected, is corrected by exchanging the bulging contour piece with the contralateral intact contour piece, which are both located between the selected crossovers. The crossovers themselves are determined in a bottom-up approach, with the shortest distance to the previous ones. The lowest and highest crossover pairs are approved by the user.

Once a reconstructed mesh is obtained from the reconstructed contour set, the region of interest is outlined, and the enclosed surface entities are retrieved (Figure 2c, right). A thin plate smoothing spline surface is then calculated only for this part of the mesh. The procedure therefore reorients the mesh region to the ground plane by calculating a central axis based on the centroids of all the slices, determining the vector which is perpendicular to this axis and which goes through the centroid of the selected region, and analysing the orientation and position of this vector. As this procedure is matrix-based, a rectangular plate is obtained first, but redundant points are easily detected since the plate outline is known. These points may be offset or even deleted, in order to emphasize the plate outline appropriately for the chosen production technique (Figure 3). Furthermore, if the reconstruction region is kown, the plate smoothing can be restricted to this region only.

Finally the plate is exported in STL format by triangulating every quadrilateral.

Results

CASE 1 - Figure 1a presents a humerus with an aneurismal bone cyst. From the 143 loaded contours, in 84 CT-slices with 1mm interslice distance, the filter procedure removed 59 small contours. Thirty-eight internal loops were corrected (first variant). Several contours contained more than one loop. For one of these contours for example, two loops contained at least 31 points – out of 392 – with start and endpoint closer than 3.5 mm and they were linearly corrected with either two or three points. The procedure did not stitch any contours but was able to remove 131 little loops and 229 small triangles. Nineteen internal loops with a length of about half the contour perimeter were removed (second variant). Finally, the third variant detected and corrected 44 middle-sized wide loops. Labelling all acceptance criteria as 'hard', no interaction was required. One contour in the defect region was reshaped manually,

ISSN: 1727-1983

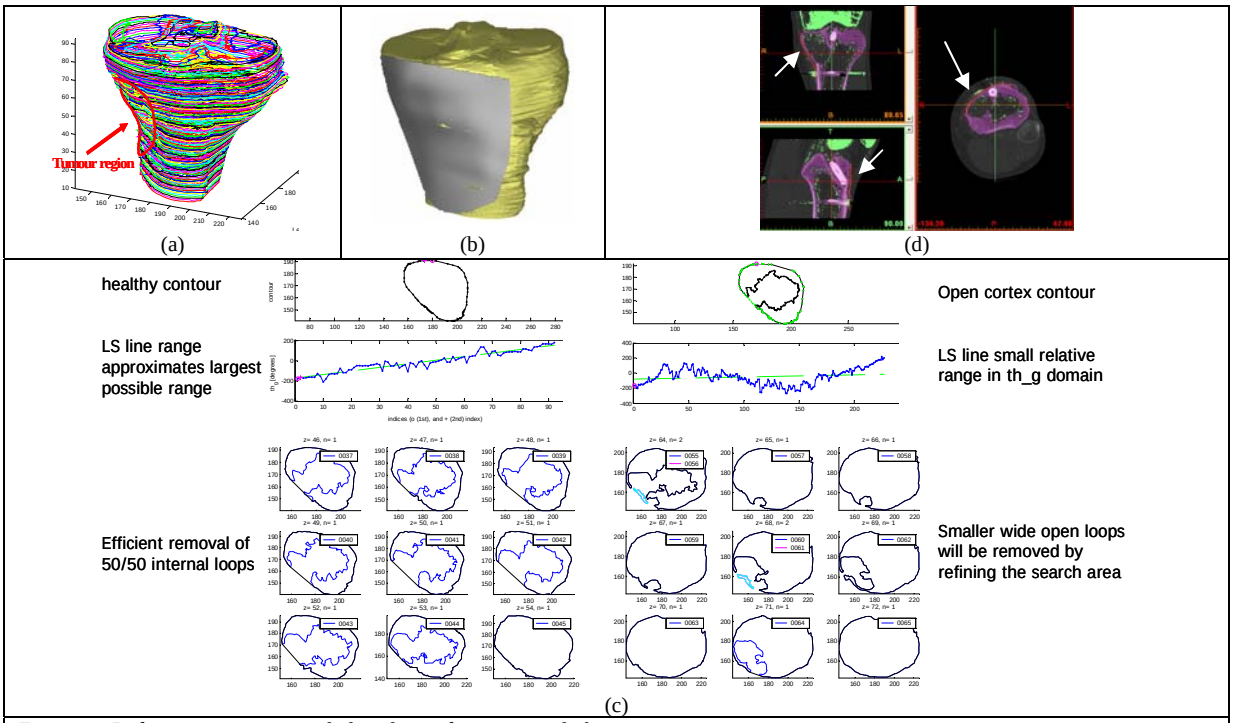

Figure 1 – Defect reconstruction and plate design for a proximal tibia tumour.
(a) Initial contour set, obtained from a quick grey-level segmentation for bone. As tumour tissue falls out of the greyvalue-range for bone, wide open internal loops are present in the bone contours.
(b) STL representations of the resulting outer cortex surface mesh and personalised reconstruction plate.
(c) Removing internal loops automatically implicates a reconstruction of the tumour defect (2nd variant).
(d) CT-data in three orthogonal views (Mimics©). The plate, indicated by the arrows, reconstructs the defect correctly and nicely fits on the sound surrounding bone.

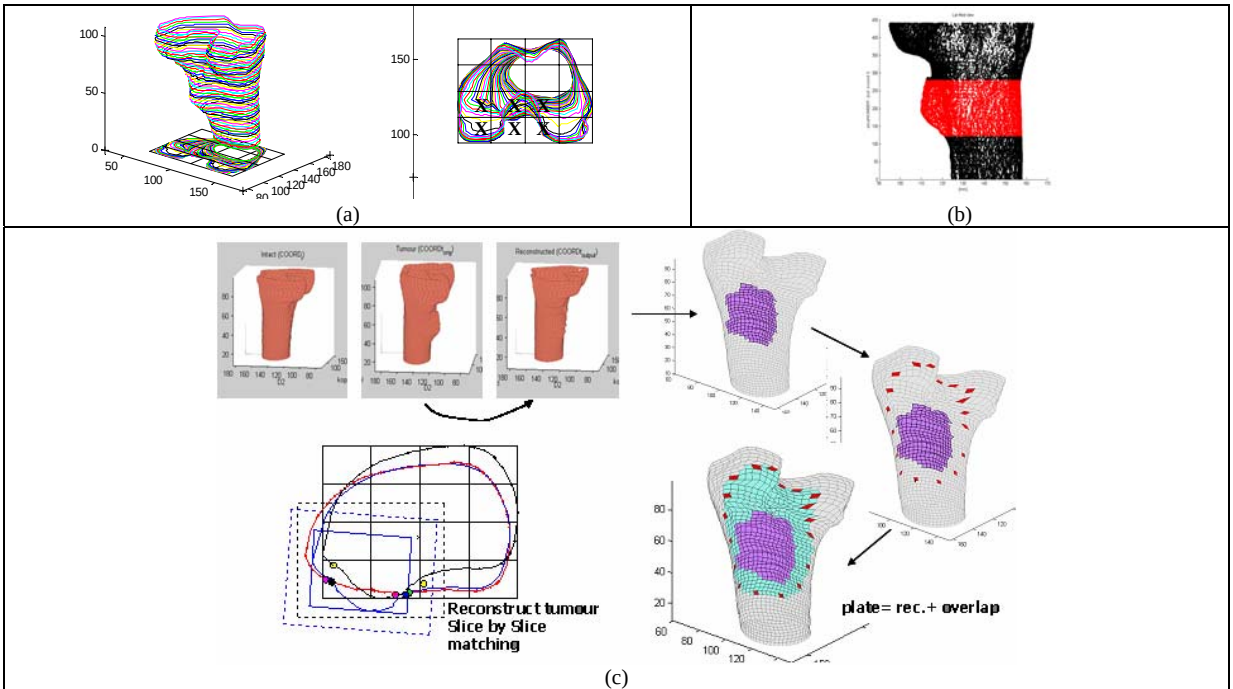

Figure 2 – Slice by slice reconstruction of a bulging contour set.
(a) The user once outlines the bulging region on an overall projection grid. The bulging region for every tumour contour is than obtained by selecting the corresponding rectangles in each contour envelope.
(b) Bulging tumour contours, which form the central portion of the plot, are detected by comparing the perimeters and the enclosed surfaces with those from the corresponding intact contours.
(c) The contralateral bone piece is mirrored. Each contour of the tumour set is matched, with its non-bulging section, to the entire corresponding intact contour. The section of the intact contour that resides between two appropriate crossovers is used to reconstruct the bulge of the tumour contour. The start and endpoints of all reconstruction segments determine a reconstructed surface region on the outer cortex mesh. The user then outlines an overlap region, which is added to the reconstruction region.

ISSN: 1727-1983

even though this was not obligatory. The default imposed accuracy between every contour point and its corresponding spline point was set to 1mm and automatically lowered for the smaller contours. The mean imposed and obtained accuracy for the splines used for the proximal tibia cortex mesh are 0.88 ± 0.15 and 0.78 ± 0.16 mm respectively. The mesh, build from fifty points per spline, represents only the outer bone surface, contains less noise and nicely covers the tumour region (Figure 1b). The uncompiled Matlab® program obtained the mesh in 20 minutes[1], from which about five minutes were used for thresholding and user interactions.

After the user outlined the membrane on the outer surface mesh, the enclosed region is retrieved, reoriented and approximated by a thin plate smoothing spline. Figure 1b demonstrates that the plate nicely fits on the STL surface mesh, which is confirmed by an overlay-view of the STL plate with the CT-data in Figure 1d.

CASE 2 - Figure 2a presents a case of a giant cell tumour in the proximal tibia, which was used by Pattijn *et al.* to demonstrate the feasibility of preformed titanium membranes for weight-bearing bone reconstructions in tumour surgery. Following the above-mentioned methodology, a surface model was built from the filtered bone contour set. The filtering performed similarly as for the tibia case, except that no large internal loops were detected and a bulging tumour was present in the mesh. From the 491 filtered contours, with a single contour per slice and 0.2 mm interpolated slice thickness, 158 contours were detected as 'bulging' and further analysed for appropriate crossovers with the corresponding mirrored contralateral contours. After five minutes of extra processing, the uncompiled Matlab® code presented the reconstructed mesh to the user, who in turn outlined the overlap region of the plate (Figure 2a-b-c). In this case, an entirely smoothed plate was preferred; depending on the offset of the border points, three representations were obtained, as illustrated in Figure 3.

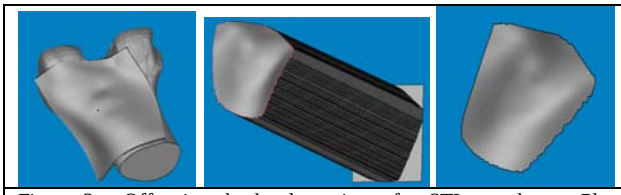

Figure 3 – Offsetting the border points of a STL membrane. Plate points that do not belong to the actual membrane can be included in the STL plate (left), included but lowered to some specified z-value (middle), or deleted (right).

[1] Calculation time using a Celeron® 2.0 GHz processor, with 512Mb of internal memory.

Discussion

Segmentation - Filtered representation. The bone representations were obtained by filter and mesh procedures which were previously developed by the author [6], since they succesfully remove shape irregularities, process bone defects for different bone types, and filter out redundant image information for the specified application. A first alternative to the adopted approach is manually segmenting the bone from CT images, but this approach is time consuming and highly user dependent. More advanced segmentation tools such as Boolean operations or region growing [Mimics®], or model based tools such as snakes or active shape models [8][9] however, are not always succesful for the mentioned application [6].

Triangulated vs. analytical model representation. As the outer surface mesh itself and all results of the platform-independent procedures have a triangulated representation, they are directly interchangeable with digital CAD and rapid prototyping software [3Matic®, Magics®, SolidView®, 3DLightyear®, FlashTLEngineer®], with the associated advantages of straightforward design and production. For comparison, analytical representations in regular CAD packages, such as NURBS surfaces, are not easy to control, encounter branching problems, sometimes inhibit straightforward CAD operations, and are problematic in case of irregular but anatomically correct bone shapes as the surface would wrinkle [10].

Surface vs. Volume model representation. The presented procedures start from an outer surface STL representation of the bone and do not use a full volume STL model representation of the skull, even though such volume STL could easily be generated in commercial medical imaging software by means of a Marching Cubes algorithm [11]. Nonetheless, for the presented applications, the outer surface presentation has some innovating advantages over a volume model.

Firstly, compared to a high resolution volume STL, an outer surface STL offers similar quality and accuracy of representation for a much smaller dataset. Compared to volume representations in the Mimicsz software for example, the presented outer surface model of the distal tibia contains 8396 triangles, which is respectively less than 35, 12, 4 and 2 percent of the total amount of triangles required for a low, medium, high and a particular custom quality volume representation.

Secondly, plate design and template deduction are *in se* completely surface based, meaning that redundant information such as inner contours and internal loops must be removed in order not to tangle automated procedures which directly retract information from the visualisation mesh. The semi-automated filter sequence was implemented to retrieve an outer surface, as it could not be obtained from a largest shell extraction from an unfiltered volume STL. The filters inherently prohibit

ISSN: 1727-1983

the polylines from penetrating the bone, and the splines are calculated to a controllable accuracy.

And thirdly, the implemented procedures have the ability to return to their 'roots', namely the bone contour representation. Contours can be adapted for reconstructions such as loop removal, reshaped to obtain smooth transitions with other contour sets, etc. Furthermore, a designer can easily switch between STL mesh and contour representation; a spline set is easily converted to an outer surface mesh and an outer surface mesh can be swiftly resliced into a reoriented contour set.

Automated tumour reconstruction – tumour hole. A contour set with middle-sized hole is automatically reconstructed by applying the filter sequence. The mesh just requires some smoothing in the defect region; no further reconstruction is needed.

Automated tumour reconstruction – tumour bulge. Manual CAD-based reshaping manipulations [2][5][3Matic[z]] are replaced by an automated sequence of selecting, matching and swapping sound and/or bulging contour points with contralateral information. This procedure is not time consuming, and moreover user-independent.

The uncompiled Matlab[y] procedure is accelerated by restricting the search for crossover to a slightly enlarged envelope around the defect region of each tumour contour (Figure 2c).

Currently, contralateral information is required for the bulge removal procedure. Since both leg are always scanned together, this data is always available, except if this information would also be distorted. Further research will therefore incorporate reference models.

Slice by slice vs. 3D tumour reconstruction. The bulge removal procedure is partly two-dimensional, thus enhancing calculation speed by matching small in-slice data sets, but runs the crossover-selection in the third direction. Full 3D ICP-matching of the reconstructed mesh with the mirrored contralateral mesh resulted in a collection of alternating surface regions, indicating that no additional or different reconstruction procedure was required.

Thin plate smoothing vs. entire mesh smoothing. Two options are available to extract a region from the mesh, either by smoothing the entire mesh and then cutting out the membrane, or vice versa. For the first option the settings of the smoothing filter, namely smoothing iterations, smooth factor, triangle reduction etc. must be well-considered and iterated as bad settings easily result in an 'inflated' and thus inaccurate mesh. A more straightforward and automated approach is obtained by first retracting the plate region, and then calculating a thin plate smoothing spline only for this part of the mesh.

Plate outline fine-tuning and validation. A main outline of a membrane can always be established, even if the surgeon cannot exactly predict the final size preoperatively. Depending on the defect type and location, trimming of the membrane can be rather extensive or on the contrary unnecessary. A resection of a bone tumour illustrates the former, a reconstruction of a shattered skull fracture or a bone augmentation the latter. In either case, the surgeon needs to plan the surgery preoperatively and the most appropriate way to do so is in close correspondence to the patients CT data, which allows a swift but nonetheless accurate validation (Figure 1d). This validation comprises the fit of the membrane on the neighbouring healthy bone - CT offers the possibility to distinguish between healthy and tumour tissue - and check whether important surrounding soft tissues, such as narrow muscle attachment regions, are preserved.

Further research will integrate soft tissue information such as important muscle attachment regions and bone thickness, directly in the surface model, thus facilitating the plate outlining.

Starting with a broad membrane region ensures a smooth transition between reconstruction region and surrounding healthy bone, and a good fit of the overlap region.

Offsetting plate border points – link with membrane production. As the plate-upsampling procedure is matrix-based, border points can be offset, resulting in three representations for the STL membrane. The production technique or the subsequent CAD operation will determine the most appropriate representation. Hydroforming, which is the current commonly used production technique for titanium membranes, requires only one die to press the titanium plate against a rubber membrane, which in turn seals an oil reservoir [2][3]. The die is obtained by materialising the virtual CAD model into a stereolithographic model (SLA) and producing a replica in synthetic hard plaster . A die which contains a clear outline of the plate border will enhance the plate after-processing stage, namely manually trimming and finishing. A plate with offset border points such as in figure 3, in the middle, would then be the most suitable.

As a CAD representation of the reconstruction membrane itself is available, time and SLA material is saved for the preparation of the hydroforming technique, and opportunities arise for *direct* production techniques. Although milling, a direct production technique, seems unfavourably due to a high loss ratio of valuable titanium, Single Point Incremental Forming (SPIF) of sheet metal could greatly decrease the production time [12]. The membrane outline could then directly be used to cut the membrane out of the formed sheet. Figure 3, on the right, presents such a representation.

Plate smoothing – entire plate or reconstruction region only. The plate extraction procedure generates a plate by upsampling the outlined mesh region. The upsampling occurs by first reorienting the selected region to the ground plane, and using a ground grid with a particular number of subdivisions. Grid points in a smoothed region are sampled from a thin plate smoothing spline, while points which lie outside of this region are sampled by linearly interpolating the mesh

ISSN: 1727-1983

points. In case of linearly upsampling, attention must be paid to the presence of non-functionalities in the point set, which would result in small 'holes' in the membrane. Finally, conversion of the plate to the STL format is easily performed by triangulating all rectangles in the grid.

A linearly upsampled overlap region can be opted if a nicely fitting overlap is sought, while a smoothed reconstruction region alone emphasises the idea of a 'freeform' reconstruction.

If no upsampling is made, thus extracting the plate region directly from the surface mesh, a good result is obtained if the mesh is sufficiently dense and smooth.

Conclusions

One general and thorough main filter procedure allows to create an easy to handle outer bone surface mesh, available in STL file format. With the filter & mesh implementations as base platform, simple straightforward solutions are generated for complex practical problems like surface based implant design and surgery planning. Middle-sized tumour holes are automatically reconstructed by applying developed mesh procedures, while bulging tumour regions are automatically reconstructed in an effective layer-by-layer approach, thereby using the mirrored contralateral bone as a guide. The former reconstruction technique has been illustrated by means of a proximal tibia tumour, the latter by means of a bulging distal femur tumour. Subsequently, both simulation cases clearly illustrated the concept of plate extraction, and the possibilities for smoothing particular plate regions, and for emphasizing the plate outline.

Acknowledgements

We express our gratitude to Dr. I Samson (Department of Orthopaedic Surgery, KU Leuven, UZ Pellenberg) for providing the CT data for the simulation cases. This research is funded by a PhD grant of the Institute for the Promotion of Innovation through Science and Technology in Flanders (IWT-Vlaanderen).

References

[1] BLACKLEY H.R., WUNDER J.S., DAVIS A., WHITE L.M., KANDEL R., and Bracale M. (1999): 'Treatment of giant-cell tumors of long bones with curettage and bone-grafting', *Surg. Am.*, **81(6)**, pp. 811-820

[2] PATTIJN V., SAMSON I., VANDER SLOTEN J., VAN AUDEKERCKE R., SWAELENS B., and DE BUCK V. (2002): 'Medical image based, preformed titanium membranes for bone reconstructions: design study and first clinical evaluation', *J. Eng.Med.*, **216**, pp. 13-21

[3] JOFFE J.M., AGHABEIGI B., DAVIES E.H., and HARRIS M. (1993): 'A retrospective study of 66 titanium cranioplasties', *British Journal of Oral and Maxillofacial Surgery*, **31**, pp. 144-148

[4] VAN STEENBERGHE D. JOHANSSON C., QUIRYNEN M., MOLLY L., ALBREKTSSON T., and NAERT I. (2003): 'Bone augmentation by means of a stiff occlusive titanium barrier - A study in rabbits and humans', *Clin Oral Implants Res*, **14(1)**, pp. 63-71.

[5] HIEU L.C., BOHEZ E., VANDER SLOTEN J., VATCHARAPORN E., BINH P.H., AN P.V., and ORIS P. (2003): 'Design for medical rapid prototyping of cranioplasty implant', *Rapid Prototyping Journal*, **9(3)**, pp. 175-186.

[6] GELAUDE F., VANDER SLOTEN J., and LAUWERS B.: 'Semi-automated segmentation and visualisation of outer bone cortex from medical images' *(submitted to Comp. Meth. in Biomech. and Biom. Eng.)*

[7] BESL P., and MCKAY N. (1992): 'A method for registration of 3-d shapes', *IEEE Transactions on Pattern Analysis and Machine Intelligence*, **14(2)**, pp. 239-256.

[8] COOTES T.F., TAYLOR C.J., COOPER D.H., and GRAHAM J. (1995): 'Active shape models – Their training and application', *Computer Vision and Image Understanding*, **61(1)**, pp. 38-59.

[9] KASS M., WITKIN A., and TERZOPOULOS D. (1987): 'Snakes: active contour models', *Int. J. Computer Vision*, **1(4)**, 321-331.

[10] GELAUDE F., PATTIJN V., VANDER SLOTEN J., and VAN AUDEKERCKE R. (2003): 'Simulation and Biomechanical evaluation of reconstructive surgery of the hip in children', Belgian Day On Biomedical Engineering 2003, Brussels, Belgium, 2003, p. 52

[11] LORENSEN W.E. and CLINE C.H. (1987): 'Marching Cubes: A High Resolution 3D Surface Construction Algorithm', *Computer Graphics*, **21(4)**, pp. 163-169

[12] DUFLOU J.R., LAUWERS B., VERBERT J., GELAUDE F., and TUNCKOL Y. (2005): 'Medical application of single point incremental forming: cranial plate manufacturing'. 2nd International Conference on Advanced Research in Virtual and Rapid Prototyping (VRAP 2005), Leiria, Portugal, 2005.

ISSN: 1727-1983